ORIGINAL ARTICLE

Protein-Loaded Solid Lipid Nanoparticles: A Novel Delivery Platform for Enhanced Bioavailability

Mallikarjuna Gandla[1], Niranjan Babu Mudduluru[2]

[1]Department of Pharmaceutical Sciences, Jawaharlal Nehru Technological University Anantapur, Andhra Pradesh, India, [2]Department of Pharmaceutical Sciences, Seven Hills College of Pharmacy, Tirupati, Andhra Pradesh, India

Abstract

Introduction: Lactoferrin (LF)-loaded solid lipid nanoparticles (SLNs) enhance LF's stability, bioavailability, and targeted anticancer activity by protecting it from degradation and enabling receptor-mediated delivery to tumor cells. This nanocarrier system offers a promising strategy for effective and safe cancer prevention and therapy. **Methodology:** A standard curve for LF was established by measuring the absorbance of serial dilutions at 465 nm, showing linearity confirmed by a high correlation coefficient (R^2) using linear regression analysis. The infrared spectra confirmed the presence of characteristic functional groups of LF, poloxamer, and the optimized formulation F6, indicating successful incorporation of both components without major structural alterations. LF-loaded SLNs were successfully formulated via homogenization–ultrasonication, producing nanosized particles (30–100 nm) with mannitol as a cryoprotectant during lyophilization. **Results and Discussion:** LF-loaded SLN formulations showed optimal entrapment efficiency (50.61–58.01%) at specific lipid and surfactant concentrations, with efficiency influenced by lipid-to-surfactant ratio and surfactant-induced surface coverage. The polydispersity index (PDI) of LF-loaded SLNs indicated narrow size distribution and good stability, with particle size and PDI increasing alongside glyceryl behenate concentration. Zeta potential analysis using Horiba SZ-100 confirmed the stability of optimized LF-loaded SLNs, with a high surface charge preventing aggregation and ensuring uniform dispersion. *In vitro* release kinetics of optimized LF-loaded nanoparticles best fit the Higuchi model ($r^2 = 0.9619$), indicating diffusion-controlled release from the lipophilic matrix. **Conclusion:** The study indicates that the nanocarrier system offers a viable and successful method for LF delivery in cancer treatment and prevention.

Key words: Anticancer activity, encapsulation efficiency, *in vitro* release kinetics, polydispersity index, zeta potential

INTRODUCTION

Lactoferrin (LF), a multifunctional glycoprotein found in milk and various secretory fluids, has shown promising anticancer properties due to its anti-inflammatory, immunomodulatory, antioxidant, and anti-proliferative actions. However, its therapeutic potential is limited by poor oral bioavailability, susceptibility to enzymatic degradation, and low stability in physiological conditions. Solid-lipid nanoparticles (SLNs) have become a viable drug delivery method for improving the bioavailability and targeted distribution of LF in cancer prevention and treatment to overcome these obstacles.[1] Biocompatible lipids make up SLNs, which are nanomicrosized carriers that stay solid at both body and room temperature. They offer several advantages, such as controlled release, improved stability of encapsulated agents, high drug loading efficiency, and the ability to bypass first-pass metabolism. When LF is encapsulated within SLNs, it is protected from degradation in the gastrointestinal tract and exhibits improved systemic circulation time and cellular uptake, especially through cancer-targeting mechanisms.[2]

Address for correspondence:
Niranjan Babu Mudduluru,
Department of Pharmaceutical Sciences,
Seven Hills College of Pharmacy, Tirupati,
Andhra Pradesh, India. Phone: +91-7702484513.
E-mail: principal.cq@jntua.ac.in

Received: 26-07-2025
Revised: 03-08-2025
Accepted: 03-08-2025

LF-loaded SLNs have demonstrated the ability to inhibit tumor cell proliferation, induce apoptosis, and suppress angiogenesis in various cancer models, including colon, breast, liver, and lung cancers. The nanoparticles also enhance LF's interaction with cancer cell membranes, promoting receptor-mediated endocytosis, particularly via transferrin or LF receptors that are overexpressed in many tumors. This targeted delivery leads to enhanced anticancer activity while minimizing damage to healthy tissues.[3] Furthermore, SLNs can be functionalized with ligands to improve site-specific targeting and can be co-loaded with other chemotherapeutic agents for synergistic effects. This approach not only maximizes LF's therapeutic potential but also reduces the side effects associated with conventional chemotherapy.[4]

Oral drug delivery is viewed as the most advantageous and safe route for the delivery of the drug, having higher patient compliance and lower cost in comparison to the parenteral route for drug delivery. Despite these elucidating traits, the therapeutic adequacy of the oral route is conspicuously exhibited.[5] Poor solubility or potentially poor permeability of the drugs adds to the fundamental causes for their poor oral bioavailability. So as to conquer the difficulties related to oral administration, nanoparticles (NPs) are seen as an option in contrast to different traditional drug deliveries, as they fundamentally tend to improve the oral bioavailability of the drugs.[6] Primer proof proposes that certain nano-pharmaceutical details may improve the intensity, safety, and efficacy of LF for a controlled drug delivery system. The success of Abraxane-albumin paclitaxel NPs has spurred recent advancements in protein-based nanomedicine, leading to the development of innovative therapeutics for the treatment of difficult illnesses such as viral infections and cancer.[7] Off-target toxicity, poor pharmacokinetics, premature drug release, and lack of precision drug targeting remain significant obstacles in the clinic, nevertheless. To get over those obstacles, different protein-based nanomedicines were created. In this sense, the glycoprotein LF, which belongs to the transferrin family, presents a promising biodegradable and well-tolerated substance that may be used as a drug nanocarrier as well as an active treatment.[8] In summary, LF-loaded SLNs represent a novel and efficient strategy for cancer prevention and treatment, offering enhanced bioavailability, targeted delivery, and improved therapeutic efficacy. Further clinical research is warranted to fully translate these findings into cancer therapies.[9]

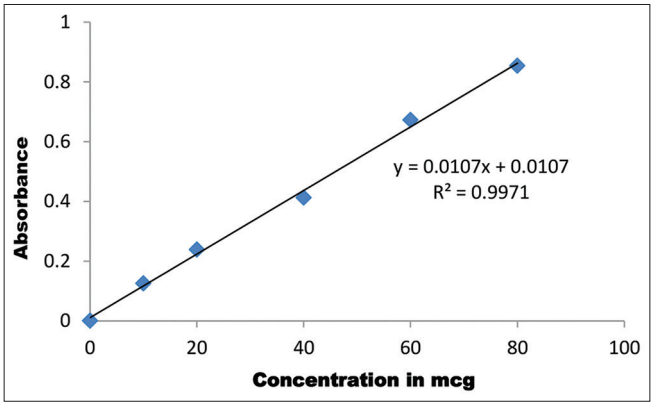

Figure 1: Calibration curve of lactoferrin in 7.4 phosphate buffer

MATERIALS AND METHODS

LF is provided as a gift sample by Sigma-Aldrich. Glyceryl behenate (GB), poloxamer 188, sodium cholate, and Span 80 were obtained from Sigma-Aldrich; Glacial acetic acid and methanol were obtained from Hi Media Laboratories.

Calibration curve of LF

10 mg of LF was dissolved in a 7.4 phosphate buffer to create a stock solution with a high concentration. 1 mL of solution from the stock solution was added to 10 mL of 7.4 phosphate buffer (100 µg/mL). 1 mL from the above solution was added to 10 mL of 7.4 phosphate buffer (10 µg/mL). A series of dilutions containing 10, 20, 40, 60, and 80 µg/mL per mL of solution were obtained by diluting the aforesaid solution with 7.4 phosphate buffer. Using a ultraviolet (UV) spectrophotometer and 7.4 phosphate buffer as a blank, the absorbance of dilutions was determined at 465 nm.[10]

FTIR spectroscopy

The LF sample was placed onto the ATR crystal and pressed down using the swivel. The contact between the sample and the swivel surface was ensured by pressing.[11] The crystal was wiped clean using a light solvent. This method is ideal for low-volume and expensive samples. The resultant spectrum is shown in Figures 2-4.

Preparation of LF SLNs

SLNs loaded with LF were effectively formulated using a homogenization and ultrasonication approach within an appropriate temperature range.[11] A hot aqueous phase containing LF and Span 80 was added to the lipid phase containing GB, poloxamer, and sodium cholate to obtain a w/o microemulsion. Homogenization time was optimized to 3 min to reduce the particle size below 1 µm using a probe sonicator.[12] The prepared microemulsion was subjected to sonication for 25 min to obtain SLNs in the range of 30–100 nm with a narrow size distribution. The SLN formulations were stored at room temperature. During lyophilization, mannitol (2%) was added, which acts as a cryoprotectant. The composition of prepared SLN

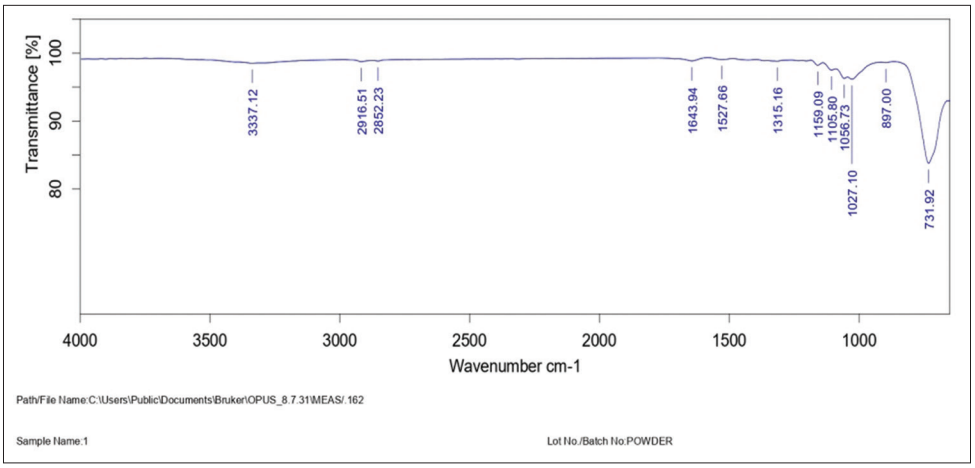

Figure 2: Infrared spectra of lactoferrin

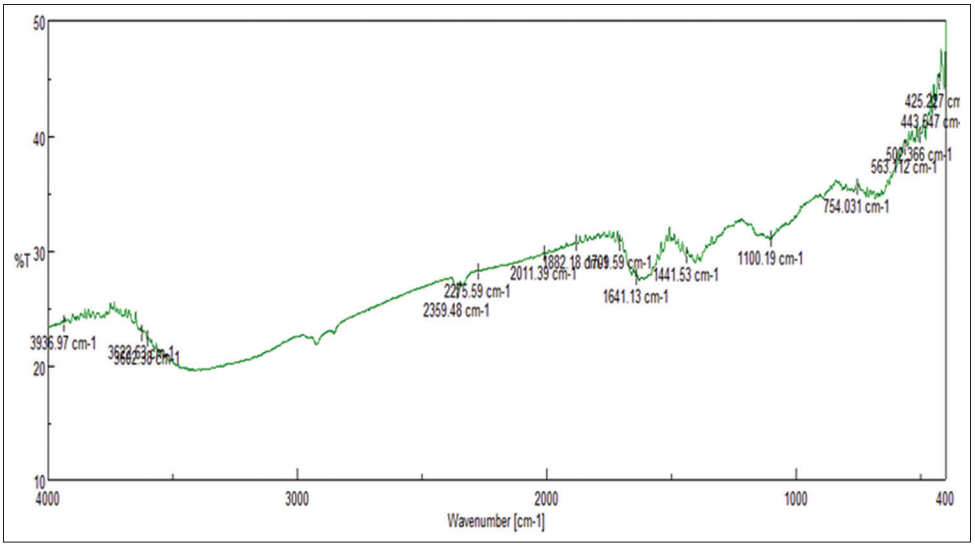

Figure 3: Infrared spectra of polaxamer 188

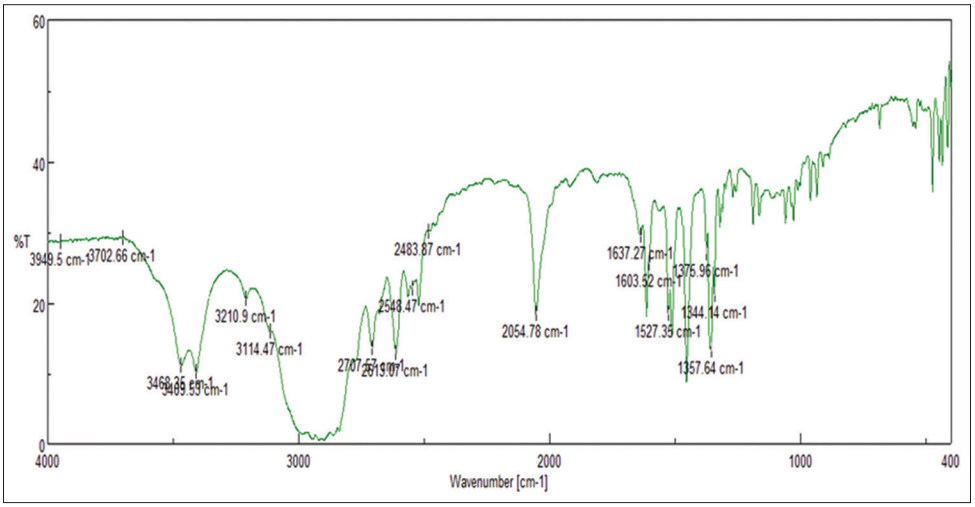

Figure 4: IR spectra of optimized formulation

batches is cited in Table 1. The formulated SLNs were evaluated for entrapment efficiency (EE), Particle size, polydispersity index (PDI), zeta potential, and *in vitro* drug release kinetics.

Table 1: Formulation of Lactoferrin solid lipid nanoparticles

Formulation Code	Ingredients				
	Lactoferrin (mg)	Glyceryl behenate (%w/w)	Poloxamer 188 (%w/w)	Sodium cholate (%w/w)	Span 80 (%w/w)
LF1	300	5	1.5	1.5	1.5
LF2	300	6	1.5	1.5	1.5
LF3	300	7	1.5	1.5	1.5
LF4	300	5	0.5	1.5	1.5
LF5	300	5	1.0	1.5	1.5
LF6	300	5	2.0	1.5	1.5
LF7	300	5	2.5	1.5	1.5
LF8	300	5	1.5	0.5	1.5
LF9	300	5	1.5	1.0	1.5
LF10	300	5	1.5	2.0	1.5
LF11	300	5	1.5	2.5	1.5

LF: Lactoferrin

Table 2: Particle size of lactoferrin powder

Peak no.	S.P. Area Ratio	Mean (nm)	S. D. (nm)	Mode (nm)
1	0.09	15.8	0.0	15.8
2	0.91	688.8	60.6	685.6
Total	1.00	629.4	199.5	685.6
Z-Average=5418.0 nm				
Polydispersity index=2.681				

Table 3: Particle size of lactoferrin-loaded solid lipid nanoparticles (LF6)

Peak no.	S. P. Area ratio	Mean (nm)	S. D. (nm)	Mode (nm)
1	0.60	10.9	1.6	10.9
2	0.40	153.8	31.2	144.1
Total	1.00	68.7	72.9	10.9
Z-Average=51.4 nm				
Polydispersity index=2.267				

Table 4: Zeta potential of lactoferrin

Peak No.	Zeta Potential (mV)	Electrophoretic mobility (cm^2/Vs)
1	−19.7	−0.000102

Table 5: Zeta potential of lactoferrin-loaded solid lipid nanoparticles

Peak No.	Zeta potential (mV)	Electrophoretic mobility (cm^2/Vs)
1	−30.4	−0.000157

In vitro drug release of lactoferrin solid lipid nanoparticle

%EE

The comparative correlation between the theoretical drug loading and the actual drug loading is EE. The solution was immediately separated in an ultracentrifuge operating at 16,000 rpm for 60 min at 4°C. With the UV spectrophotometer set to 465 nm, the amount of LF in the obtained clear supernatant sample was calculated.[13] Based on the value of the highest %EE, the prepared NPs were selected as optimized, and further characterization will be continued. These optimized NPs will be identified and selected for further studies.

Particle size

The Horiba Scientific SZ-100 with dynamic laser light scattering technology was utilized to measure the PDI and mean particle size for the optimized NPs based on their highest %EE. Before the dispersions were tested at a 90° angle, they were diluted 100 times with deionized water.[14] An indication of particle size distribution PDI was calculated. PDI lying in the range 0.15–0.3 specifies uniformity of size, whereas a PDI value above 0.3 demonstrates heterogeneity in the particle size. If the value is 0.3, it indicates excellent particle size, and a value of 0 indicates all particles are of the same size.

Zeta potential

Zeta potential values indicate the stability of a NP by measuring the surface charge, which determines the repulsive forces between particles, preventing them from clumping together and ensuring their dispersion in a liquid medium. A high zeta potential signifies a stable NP dispersion, whereas a low zeta potential leads to aggregation and instability. The

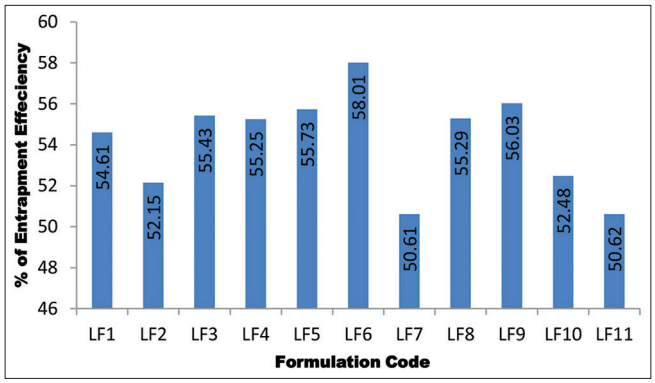

Figure 5: Encapsulation efficiency of lactoferrin solid lipid nanoparticles

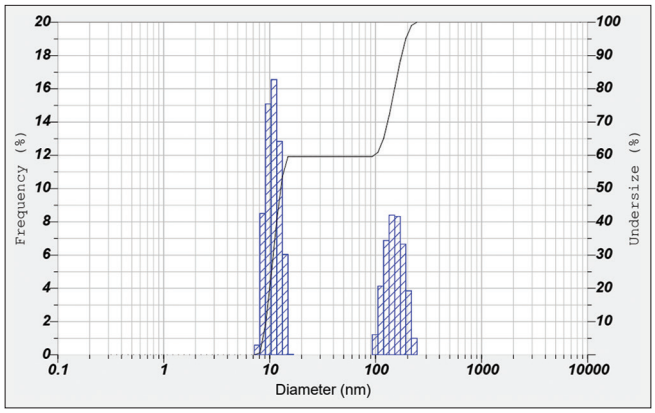

Figure 6: Particle size of powder lactoferrin

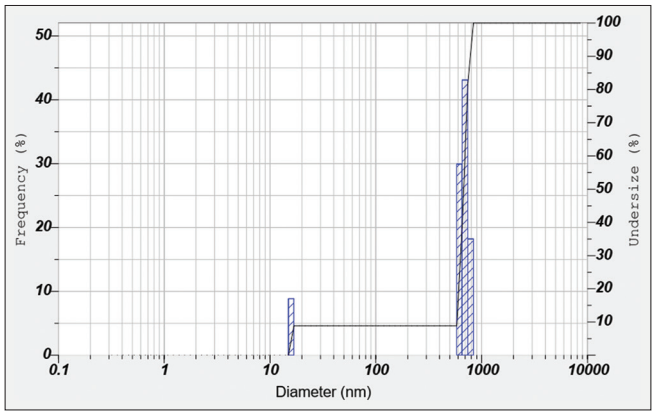

Figure 7: Particle size of lactoferrin (LF) loaded solid lipid nanoparticles (LF6)

Horiba scientific SZ-100 was used to calculate the ZP of optimized NPs based on their highest %EE, using the laser light scattering technique. To suitably dilute the mixture, double-distilled water was used. A 90° angle was used to take the measurements.[15]

In vitro drug release studies

Modified USP dissolution apparatus 1 with a two-sided open glass cylinder was used to check the *in vitro* drug release,

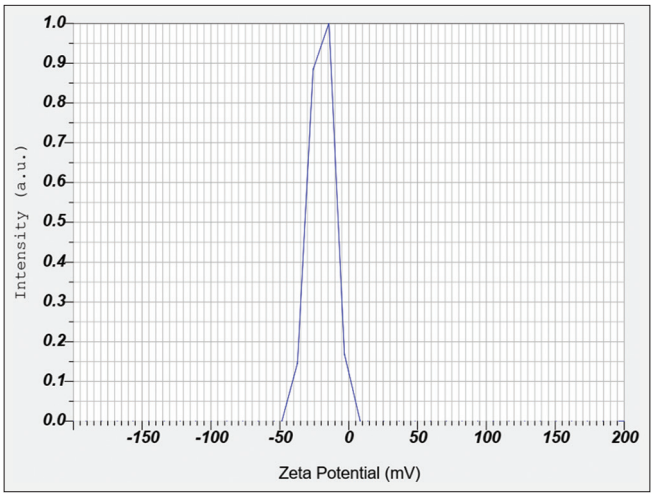

Figure 8: Zeta potential of lactoferrin

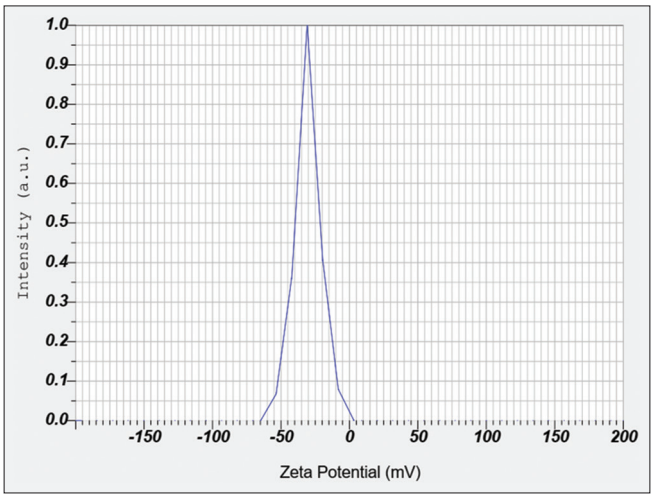

Figure 9: Zeta potential of lactoferrin solid lipid nanoparticles

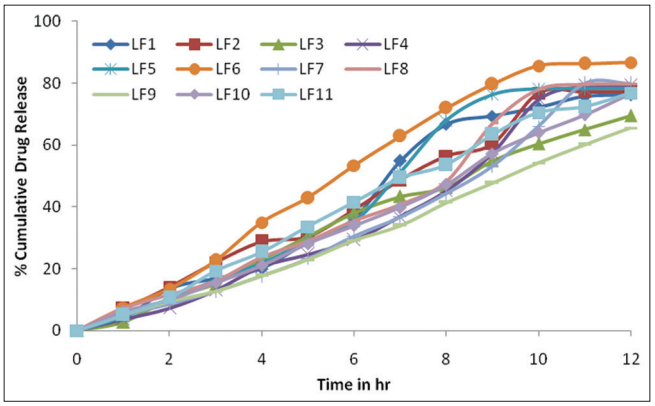

Figure 10: *In vitro* drug release of lactoferrin solid lipid nanoparticle

which was set at a temperature of 37±0.5°C, and the study was done for 12 h. Dialysis membrane, molecular weight of around 12000–14000 A° (Himedia, Mumbai) was used as a diffusion barrier. The glass cylinder was fixed on the stirrer, and 5 mL of solid lipid NP was introduced from the open side. A phosphate buffer of pH 7.4 maintained at a temperature

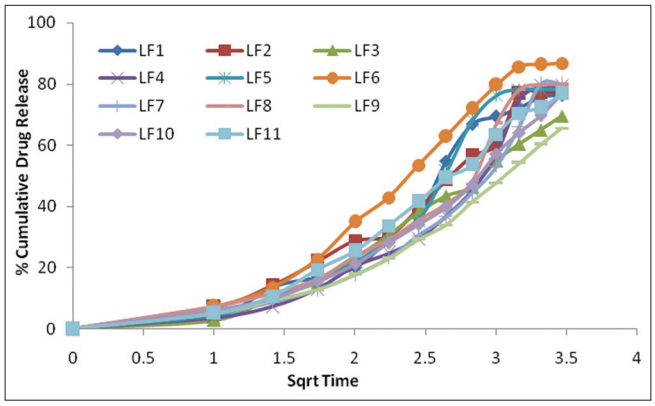

Figure 11: Higuchi kinetic profile of lactoferrin solid lipid nanoparticle

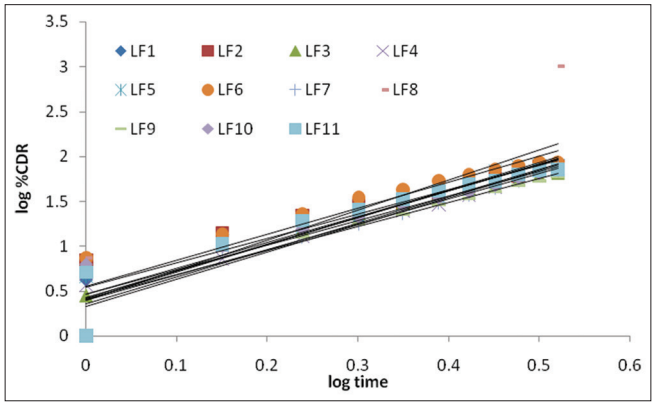

Figure 12: Korsmeyer–Peppas profile of lactoferrin solid lipid nanoparticle

of 37°C±0.5°C was used as the dissolution medium, and the stirrer was suspended in it, which was allowed to rotate at a speed of 100 rpm. A small part of the samples was withdrawn at a pre-determined interval, and volume was made up with the phosphate buffer. Drug release was then analyzed by measuring the samples for absorbance at 465 nm by the UV-visible spectrophotometer, and is represented in Figure 10.[16]

RESULTS AND DISCUSSION

Calibration curve of LF

The calibration curve graph for Lactoferrin shows a strong linear relationship between concentration and response, with a regression coefficient (R^2) of 0.997 depicted in Figure 1. This high value indicates excellent linearity and reliability of the method, confirming its suitability for accurate quantification of Lactoferrin within the tested concentration range.

FTIR spectroscopy

Interpretation of infrared (IR) spectrum of LF showed N-H stretch at 3446, 3396, C≡C stretch at 2056, C=C alkene at 1650, 1621, C=C aromatic at 1532, 1521, interpretation of IR spectrum of poloxamer showed OH at 3385.09, NH_2 at 3277.08-3223.13, CH_3, CH_2 at 2992.30-2957.65, NH_2 at 2830.87 and interpretation of IR spectrum of optimized formulation F6 showed N-H stretch at 3446, 3396, C≡C stretch at 2056, C=C alkene at 1650, 1621, C=C aromatic at C=C aromatic, OH at 3385.09, NH_2 at 3277.08-3223.13, NH_2 at 2830.87 in Figures 2-4, respectively.

Encapsulation efficiency of LF SLNs

The designed formulations showed moderate-to-high LF EE in the range of 50.61–58.01 % (w/w). The impact of the concentration of lipid on EE was studied by maintaining the amount of surfactant while varying the amount of lipid. The findings demonstrated that entrapment effectiveness declined with increasing lipid content. It was found experimentally that the EE was optimal at 5% lipid, 1.5% (w/w) poloxamer 188, and 1.5% (w/w) sodium cholate, respectively. The LF EE was significantly decreased with increasing the amounts of poloxamer 188 and sodium cholate in the formulations, respectively, as depicted in Figure 5. In the batches of SLN formulations, the increased concentration of surfactant led to increased surface coverage on the NPs, which in turn resulted in increased EE, hence preventing leaching of the drug from the matrix.[17]

Particle size and PDI

PDI data of various formulations of LF-loaded SLN with varying concentrations of GB, poloxamer188, and sodium cholate are depicted in Figures 6 and 7, indicating a narrow size distribution pattern, further revealing higher stability of the SLNs. It is evident that the particle size and PDI of SLN increase with an increase in the GB content in the final dispersion as depicted in Tables 2 and 3.

Zeta potential

The zeta potential of Lactoferrin (-19.7 mV) and its solid lipid nanoparticles (-30.4 mV) indicates increased surface charge upon nanoparticle formulation and showed in table 4 & 5. The higher negative zeta potential of the nanoparticles suggests improved stability due to greater electrostatic repulsion, reducing aggregation and enhancing their suitability for drug delivery applications were represented in Figures 8 and 9.

Release kinetic studies

To examine the release kinetics from optimized LF-loaded NPs, the *in vitro* release data were analyzed using three mathematical models: The coefficients of regression (r^2) for the zero order, first order, Hughchi, and Korsmeyer–Peppas models were calculated from Figure 10.

The greatest r^2 value of 0.9619. This suggests a direct correlation between a protein's concentration and rate of release. The LF release rate can be described as either independent or dependent on its concentration using the zero and first order, respectively. The release of LF from a lipophilic matrix can be explained by the Higuchi model and the Korsmeyer–Peppas model and represented in Figures 11 and 12.[18]

CONCLUSION

The effective development of LF-loaded SLNs using homogenization–ultrasonication produced stable, nanoscale formulations with improved bioavailability and specific anticancer potential. Characterization confirmed efficient drug entrapment, structural integrity, narrow particle size distribution, and high zeta potential, indicating good stability. The *in vitro* release followed Higuchi kinetics, suggesting diffusion-controlled drug release. Overall, this nanocarrier system presents a promising and effective strategy for LF delivery in cancer prevention and therapy. All the ingredients showed compatibility with suitable physical and chemical techniques. Based on the highest value of % EE, the LF6 is selected as the optimized one and performed particle size, ZP, FTIR spectroscopy, and *in vitro* drug release. The optimized LF6 poses the average particle size of 100 nm, ZP of −122.6 mV, and FTIR reveals no significant interaction between the LF and excipients used in the study.

CONFLICT OF INTEREST

Nil.

REFERENCES

1. Kasimedu S, Selvam UH, Sharma KS, Arrivur NS, Mudduluru NB. Mesoporous silica nanoparticles: A promising portal for diagnosis and treatment for chronic diseases. Indian J Pharm Educ Res 2025;59:S776-87.
2. Pamlenyi K, Regdon G Jr., Jojart-Laczkovich O, Nemes D, Bacskay I, Kristo K. Formulation and characterization of pramipexole containing buccal films for using in Parkinson's disease. Eur J Pharm Sci 2023;187:106491.
3. Arpa MD, Okur NU, Gok MK, Ozgumuş S, Cevher E. Chitosan-based buccal mucoadhesive patches to enhance the systemic bioavailability of tizanidine. Int J Pharm 2023;642:123168.
4. Thulluru A, Mahammed N, Shakir Basha S, Mohan KS, Kumar CS, Saravanakumar K. Effect of enzyme dependent polymers on the release profile of press coated esmeprazole colon targeted tablets. Res J Pharm Technol 2020;13:6186-94.
5. Gaber DA, Alburaykan AI, Alruthea LM, Aldohan NS, Alharbi RF, Aljohani AR, *et al*. Development, *in vitro* evaluation, and *in vivo* study of adhesive buccal films for the treatment of diabetic pediatrics via trans mucosal delivery of gliclazide. Drug Des Devel Ther 2022;31:4235-50.
6. Kasimedu S, Battaluri RN, Pommala N, Mudduluru NB, Gandla M, Vadamala PR. Solid lipid nanoparticles in drug delivery: Bridging tradition and innovation. Future J Pharm Health Sci 2025;5:86-96.
7. Hassan AA, Kristo K, Ibrahim YH, Regdon G Jr., Sovany T. Quality by design-guided systematic development and optimization of mucoadhesive buccal films. Pharmaceutics 2023;15:2375.
8. Kasimbedu S, Chella S, Bharathi T, Pommala N, Mannepalli DS. A piroxicam inclusion complexation for solubility enhancement: Design and development. J Young Pharm 2022;14:192-7.
9. Samanthula KS, Mahendra Kumar CB, Bairi AG, Satla SR. Development, *in vitro* and *ex-vivo* evaluation of muco-adhesive buccal tablets of hydralazine hydrochloride. Braz J Pharm Sci 2022;58:e18635.
10. Medabalimi M, Saravanakumar K, Satyanarayana SV. Development and validation of stability indicating RP-UPLC method for quantitative estimation of safinamide mesylate in bulk and its tablet dosage form. Curr Trends Biotechn Pharm 2022;16:50-9.
11. Chella S, Kasimedu S, Pommala N, Thulluru A, Gandla M, Vadamala PR. Chitosan nanoparticles enhance permeability of rizatriptan in mucoadhesive buccal films: A promising approach for improved drug delivery. Res J Pharm Technol 2025;18:1308-16.
12. Mohammed MF, Sadeq ZA, Salih OS. Formulation and evaluation of mucoadhesive buccal tablet of Anastrozole. J Adv Pharm Educ Res 2022;12:38-44.
13. Reddy KT, Dharmamoorthy G, Devi DV, Vidiyala N, Bagade OM, Kasimedu S, *et al*. Phytoconstituent-based green synthesis of nanoparticles: Sources and biomedical applications in cancer therapy. Asian J Green Chem 2025;9:329-54.
14. Mady O, Hussien S, Abdelkader DH, El-Dahaby E. Metoclopramide loaded buccal films for potential treatment of migraine symptoms: *In vitro* and *in vivo* study. Pharm Dev Technol 2023;28:650-9.
15. Sharma MK, Pokhariyal T, Mehta A, Kasimedu S, Kumar V, Kiran S, *et al*. Development and evaluation of methotrexate nanostructured lipid carriers for topical treatment of atopic dermatitis. Afr J Biol Sci 2024;6:451-61.
16. Panchal P, Srivastava S, George M, Anjum N, Parvez N. Formulation and evaluation of buccal film of rabeprazole sodium. Res J Pharm Technol 2023;16:2297-300.
17. Mehta HD, Kasimedu S, Bharath Raj KC, Kiran V. Optimizing orphan drug rucaparib transdermal patches for ovarian cancer: A design expert-based strategy for prolonged drug release. Int J Drug Deliv Technol 2024;14:1441-9.

18. Zewail MB, Asaad GF, Swellam SM, Abd-Allah SM, Hosny SK, Sallah SK, *et al*. Design, characterization and *in vivo* performance of solid lipid nanoparticles (SLNs)-loaded mucoadhesive buccal tablets for efficient delivery of lornoxicam in experimental inflammation. Int J Pharm 2022;624:122006.

Source of Support: Nil. **Conflicts of Interest:** None declared.